An accurate equation of state for the one-component plasma in the low coupling regime

2010 J. Phys. A: Math. Theor. 43 105501

(http://iopscience.iop.org/1751-8121/43/10/105501)

J. Phys. A: Math. Theor. **43** (2010) 105501 (18pp) doi:10.1088/1751-8113/43/10/105501

An accurate equation of state for the one-component plasma in the low coupling regime

Jean-Michel Caillol[1] **and Dominique Gilles**[2]

[1] Laboratoire de Physique Théorique, CNRS (UMR 8627), Bât. 210, Université de Paris-Sud, 91405 Orsay Cedex, France
[2] CEA/DSM/Institut de Recherche sur les lois Fondamentales de l'Univers, CE Saclay, 91191 Gif sur Yvette Cedex, France

E-mail: Jean-Michel.Caillol@th.u-psud.fr and Dominique.Gilles@cea.fr

Received 30 September 2009, in final form 10 January 2010
Published 17 February 2010
Online at stacks.iop.org/JPhysA/43/105501

Abstract
An accurate equation of state of the one-component plasma is obtained in the low coupling regime $0 \leqslant \Gamma \leqslant 1$. The accuracy results from a smooth combination of the well-known hypernetted chain integral equation, Monte Carlo simulations and asymptotic analytical expressions of the excess internal energy u. In particular, special attention has been brought to describe and take advantage of finite size effects on Monte Carlo results to get the thermodynamic limit of u. This combined approach reproduces very accurately the different plasma correlation regimes encountered in this range of values of Γ. This paper extends to low Γ's, an earlier Monte Carlo simulation study devoted to strongly coupled systems for $1 \leqslant \Gamma \leqslant 190$ (J-M Caillol 1999 *J. Chem. Phys.* **111** 6538). Analytical fits of $u(\Gamma)$ in the range $0 \leqslant \Gamma \leqslant 1$ are provided with a precision that we claim to be not smaller than $p = 10^{-5}$. The hypernetted chain equation and exact asymptotic expressions are shown to give reliable results for $u(\Gamma)$ only in narrow Γ intervals, i.e. $0 \leqslant \Gamma \lesssim 0.5$ and $0 \leqslant \Gamma \lesssim 0.3$ respectively.

PACS numbers: 52.65.−y, 52.25.Kn, 52.27.Aj

(Some figures in this article are in colour only in the electronic version)

1. Introduction

The aim of this paper is to obtain the equation of state (EOS) of a plasma in the low coupling regime with a high precision. In this regime standard Monte Carlo (MC) and Molecular Dynamics simulation techniques must be handled with care due to huge finite size effects and, on the other hand, the ideal gas approximation or more elaborated analytical expressions commonly used are valid only, but asymptotically, for very small values of the coupling

parameters. Such thermodynamic conditions are relevant for many astrophysical or laboratory plasmas' hydrodynamics applications.

However, we shall restrict ourselves to the well-known one-component plasma (OCP) model, which consists of identical point ions, with number density n, charges Ze, moving in a neutralizing background, electrons for instance, where $n = N/\Omega$, N being the number of particles and Ω being the volume of the system [1]. In the very low coupling regime, the virial expansion supplemented by well-documented resummation methods, as the well-known Debye–Hückel (DH) theory [2] and its extensions (see e.g. Cohen [3] and, more recently, Ortner [4] expansions for instance) give reliable results. In the low to intermediate coupling regimes the hypernetted chain (HNC) integral equation [5] must be solved numerically. In the strong correlation regime, the OCP has also been extensively studied by Monte Carlo and molecular dynamics simulations for three decades, see e.g. [1, 6–12] and references cited herein. Finally, overall fits of all these data spreading in the range $0 \leqslant \Gamma \leqslant 190$ have been given in [13].

In [11] one of us has determined the thermodynamic limit of the excess internal energy per particle $u_{N=\infty}$ of the OCP with a high precision by means of MC simulations in the canonical ensemble within hyperspherical boundary conditions [10, 11] for $1 \leqslant \Gamma \leqslant 190$. We recall that in the thermodynamic limit, i.e. for an infinite system of particles, the thermodynamics properties of the model depend solely on the coupling parameter $\Gamma = \beta(Ze)^2/a_i$ ($\beta = 1/kT$, k being the Boltzmann constant, T being the temperature and a_i being the ionic radius defined by $4\pi n a_i^3/3 = 1$), whereas, for a finite sample, an additional dependence on the number of particles N remains. In paper [11], henceforth to be referred to as 'I', special attention has been brought to describe and take advantage of such finite size effects on the energy $u_N(\Gamma)$ to get its thermodynamic limit $u_{N=\infty}$, using all facilities of work stations available at that time.

Recently we have also performed extensive MC simulations of the related Yukawa one-component plasma (YOCP), i.e. a system made of N identical point charges Ze interacting via an effective Yukawa pair-potential $v_\alpha(r) = (Ze)^2 \exp(-\alpha r)/r$, where α is the so-called screening parameter [14], not to be discussed however in this work. For the OCP and the YOCP as well, in the low Γ regime, the Debye length (i.e. the correlation length associated with charge fluctuations) becomes of the order or much larger than the size of the simulation box, yielding huge finite size effects on $u_N(\Gamma)$. Therefore and despite these numerous studies and amount of work, it appears that it is impossible to determine a smooth combination of all data coming from various techniques and this can affect hydrocode applications in the regime $\Gamma \leqslant 1$. A precision of one part in 10^4 as that available in already published works is indeed not sufficient to assess the validity of approximate schemes (HNC, low-coupling expansions).

With today's computers it is now possible to explore this range of small Γ values with the help of performant simulation techniques and to obtain such precise results, at least up to one part in $\sim 10^5$, so that they can be considered as the *reference* ones to be used in many applications dealing with degenerate astrophysical or laboratory plasmas.

We also examine carefully in this paper the connection between MC and first principle analytical or HNC results for $\Gamma \leqslant 1$. We have thus explored and precised the domain of validity of each of these methods. It turns out to be necessary to combine all of these approaches to obtain a continuous representation of $u_{N=\infty}(\Gamma)$ in the range $0 \leqslant \Gamma \leqslant 1$. Finally we extract from these combined approaches the best possible analytical representation for $u_\infty(\Gamma)$.

Our paper is organized as follows. The next section is devoted to a brief presentation of the main features of low Γ expansions (section 2.1), the HNC integral equation (section 2.2) and the rather unusual but efficient MC technique used in this paper (section 2.3). Note that we have redone, by passing, extremely accurate HNC calculations and obtained new fits of HNC data, presented in section 2.2. In section 3, we present and discuss our MC simulations.

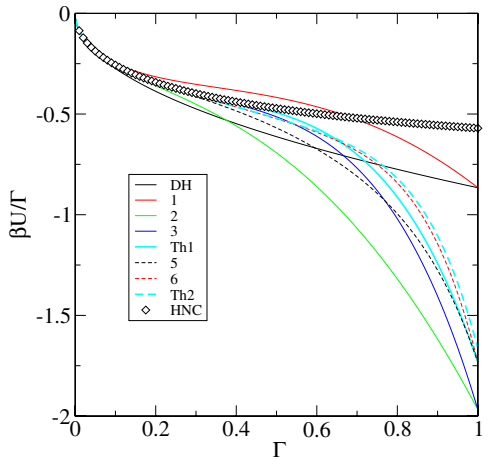

Figure 1. Reduced excess energy $\beta u/\Gamma$ versus $0 \leqslant \Gamma \leqslant 1$. Diamonds: HNC, black solid line: DH, thick grey solid line: Th1 approximation (2.1*a*), thick grey dashed line: Th2 approximation (2.1*b*) and other curves represent the successive orders of expansion (2.1).

Fits of the data are described in detail and widely illustrated. Finally conclusions are drawn in section 4.

2. Low Γ calculation methods

The interval $0 \leqslant \Gamma \leqslant 1$ covers various correlation regimes from no correlation ($\Gamma = 0$, i.e. the ideal gas) to an intermediate correlated regime ($\Gamma = 1$, no oscillation or structure in the pair correlation functions). In any case, the long-range nature of the interaction potential between two ionic charges causes Mayer graphs to diverge [1]. A field theoretical diagrammatic representation of cluster integrals has been proposed recently in [4] to avoid complicated chain resummations in an attempt to treat the Γ expansion of the classical Coulomb system in a more controlled and systematic way. In this interesting paper the final expansion obtained by the author improves earlier and seminal analytical results of Cohen *et al* [2, 3] obtained by traditional diagrammatic expansions and resummations. From these theoretical analyses it turns out that the physics in this small interval $0 \leqslant \Gamma \leqslant 1$ is extremely complicated and exhibits many different correlation regimes, even more than in the widely studied region $1 \leqslant \Gamma \leqslant 190$ [1, 6–11]. The low Γ expansions obtained by Cohen *et al* and Ortner for $u_\infty(\Gamma)$ converge to the HNC results only for $0 \leqslant \Gamma \leqslant 0.2$ as apparent in figure 1. For higher values of Γ these asymptotic expressions do not seem to converge at all and, moreover, the high-order terms of the expansions do not improve the results of the lower orders. Anticipating the results of sections 2.2 and 2.3 and, as can be observed in figure 2, the HNC data deviate from our MC results as soon as $\Gamma \geqslant 0.5$. It results from this sketchy discussion that we must distinguish three different regimes of correlations in the interval $0 \leqslant \Gamma \leqslant 1$, and we confess that this complexity motivated the present study.

2.1. Cohen and Ortner analytical expansions

In [4] Ortner has developed an effective method based on the Hubbard–Stratonovich (HS) transformation and field theoretical approaches to calculate the free energy of classical

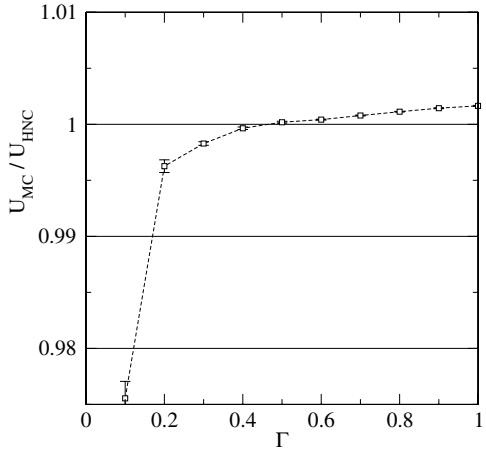

Figure 2. Ratio of MC excess energies extrapolated to their thermodynamic limit (see section 3.3) to HNC results versus Γ in the low coupling regime.

Coulomb systems in the low-Γ regime [15–17]. The HS transform was used to obtain the EOS of a classical plasma and notably that of the OCP. The non-trivial part of the Helmholtz free-energy density was derived up to order Γ^6, improving on the previous results of Cohen *et al* at order $\Gamma^{\frac{9}{2}}$, obtained by a method of resummation of diverging diagrams. The author gives an analytical representation of the excess internal energy βu of the OCP, valid at low Γ, however, without any estimation of the error. It reads

$$\beta u(\Gamma) = p_0\Gamma^{3/2} + p_1\Gamma^3 \ln\Gamma + p_2\Gamma^3 + p_3\Gamma^{9/2}\ln\Gamma + p_4\Gamma^{9/2} \tag{2.1a}$$

$$+ p_5\Gamma^6 \ln^2\Gamma + p_6\Gamma^6 \ln\Gamma + p_7\Gamma^6 \tag{2.1b}$$

with the constants, $p_0 = -\sqrt{3}/2$, $p_1 = -9/8$, $p_2 = -(9\ln 3)/8 - 3\,C_E/2 + 1$, $p_3 = -(27\sqrt{3})/16$, $p_4 = 0.2350$, $p_5 = -81/16$, $p_6 = -2.0959$, $p_7 = 0.0676$ and $C_E = 0.577\,215\,66$ the Euler constant. Expression (2.1) (to be referred to as Th2 henceforth) improves on that given by Cohen *et al* (to be referred to as Th1 henceforth) [3], which corresponds to line (2.1*a*), while the additional terms are those of line (2.1*b*). We recognize that the first term ($-\sqrt{3}\Gamma^{3/2}/2$) is exactly the well-known Debye–Hückel (DH) contribution. Figure 1 displays the results of the reduced excess energy $\beta u/\Gamma$ versus Γ at successive orders in the Γ expansion (2.1). A close examination of the figures reveals that the DH approximation is nearly exact up to $\Gamma = 0.05$, in the sense that higher order contributions do not change the result. A comparison with HNC results, which are supposed to be nearly exact at least up to $\Gamma = 0.5$ (this point will be fully discussed in the next section), shows the convergence of the expansions Th1 and Th2 to HNC at $\Gamma \leqslant 0.3$ and $\Gamma \leqslant 0.2$ respectively. However we do not observe any trend of convergence of these expansions for $\Gamma \geqslant 0.4$. We also note that the additional terms given by Ortner (cf equation (2.1*b*)) lead to a crossing of the curves rather than to an improved convergence. We suspect either some misprints in the reported p_n for $n = 5, 6, 7$, since the Γ functional dependence of (2.1) is undoubtedly correct, or some problems linked with nasty mathematical properties of the series (i.e. asymptotic convergence, small radius of convergence, etc).

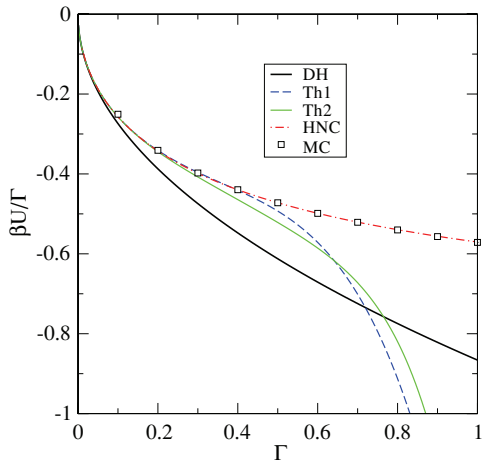

Figure 3. Reduced excess energy $\beta u/\Gamma$ versus Γ. Squares: MC (the symbols are larger than error bars), black solid line: DH, dashed dotted line: HNC, dashed grey line: Th1 approximation (2.1*a*) and solid grey line: Th2 approximation (2.1*b*).

2.2. The HNC method and fits

2.2.1. Method. We have recalculated high precision HNC calculations for a hundred of values of Γ in the range (0, 1) (see figures 1 and 3); additional calculations were also carried out for some higher values of the coupling parameter, in the range $1 \leqslant \Gamma \leqslant 10$, see figure 4. We used the NG method [5] with the following control parameters: the pair correlation functions (direct and non-direct respectively) $c(r)$ and $h(r)$, as well as their Fourier transforms $\widetilde{c}(k)$ and $\widetilde{h}(k)$, were tabulated on grids of $N = 2^M$ points with $M = 20$ in order to make use of fast Fourier transforms with intervals of $\Delta r = 0.001$ and $\Delta k = 2\pi/N \simeq 6 \times 10^{-3}$ in direct and Fourier space respectively. The dimensionless energies were computed according to the formulae [1]

$$\frac{\beta u^{(r)}}{\Gamma} = \frac{3}{2} \int_0^\infty \mathrm{d}r\, r h(r), \tag{2.2a}$$

$$\frac{\beta u^{(k)}}{\Gamma} = \frac{3}{2\,(2\pi)^2} \int_0^\infty \mathrm{d}k\, \widetilde{h}(k), \tag{2.2b}$$

where the distances 'r' are measured in the units of the ionic radius a_i and the wave numbers k in units of a_i^{-1}. The comparison of these two estimations $u^{(r)}$ and $u^{(k)}$ of the energy, which of course should be equal, gives an idea on the relative precision of the numerical resolution of HNC, typically about 10^{-12} at $\Gamma = 0.01$ and 10^{-13} at $\Gamma \geqslant 0.1$. Another useful test is to check the Stillinger–Lovett (SL) sum rules; recall briefly the two first SL rules (the third one should not be satisfied by HNC [1, 19])

$$3 \int_0^\infty \mathrm{d}r\, r^2 h(r) = -1, \tag{2.3a}$$

$$3 \int_0^\infty \mathrm{d}r\, r^4 h(r) = \frac{2}{\Gamma}. \tag{2.3b}$$

With the control parameters given above, the SL rules were satisfied with a relative precision of about 10^{-13}.

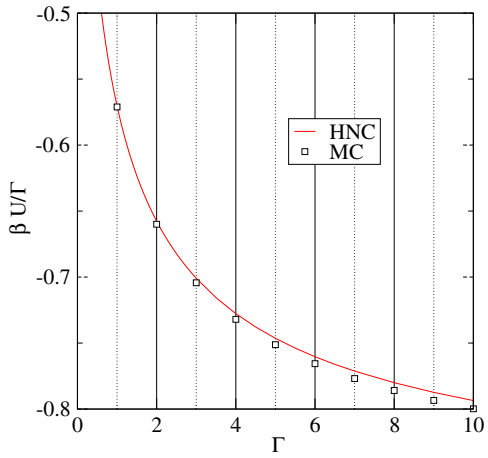

Figure 4. Comparison between HNC (line) and MC data (squares, present work and previous results, see [11]) for the reduced excess energy $\beta U/\Gamma$ versus $1 \leqslant \Gamma \leqslant 10$.

Table 1. First five Cohen–Ortner coefficients (cf equation (2.1), first line) compared to the correspondent coefficients of the fits of the energy $\beta u(\Gamma)/\Gamma$ for HNC and MC data. Second line: HNC, seven parameters, $p_0 = -\sqrt{3}/2$ fixed to its DH value. Third line: HNC, eight parameters. Last line: MC data in the range $0.4 \leqslant \Gamma \leqslant 1$, five parameters ($p_5 = p_6 = p_7 = 0$).

p_0	p_1	p_2	p_3	p_4	Method
−0.866 025 4038	−1.125 000 0000	−1.101 766 2315	−2.922 835 7378	0.235 000 0000	Ortner
−0.866 025 4038	−1.112 764 5260	−1.063 607 5255	−3.196 017 7420	−1.423 681 0385	HNC-DH
−0.865 850 9448	−1.096 735 8264	−1.022 452 3661	−2.976 570 9164	−1.186 113 3643	HNC
−0.840 902 5523	−0.519 839 1670	−0.000 198 5314	−0.140 213 2305	0.269 708 1277	MC

Table 2. Same as in table 1 for the last three parameters p_5, p_6 and p_7 of the fit of HNC data.

p_5	p_6	p_7	Method
−5.062 500 000	−2.095 900 0000	0.067 600 0000	Ortner
0.586 872 5967	−2.198 270 0902	2.782 859 9024	HNC-DH
0.509 323 9388	−1.953 186 0886	2.503 962 0685	HNC

2.2.2. Fits. We used the functional form of Ortner asymptotic expression (2.1) to fit the HNC data for $\beta u/\Gamma$ in the interval $0 \leqslant \Gamma \leqslant 1$. We are left with an eight parameters fit (i.e. the p_i for $i = 0, \ldots 7$), or a seven parameters fit if p_0 is fixed to its Debye value $p_0 = -\sqrt{3}/2$. The values found for the p_i are given in tables 1 and 2. For the eight parameters fit, the maximum deviation of the fit from the HNC data is 7.3×10^{-7} with a mean deviation of 1.9×10^{-7}, while for the seven parameters fit these deviations are 1.3×10^{-6} and 3.3×10^{-7} respectively. Some comments are in order.

- First, for $\Gamma \leqslant 0.1$, the estimations of $\beta u/\Gamma$ in the framework of HNC, Cohen *et al* and Ortner theories all coincide with an absolute precision of the order of 1×10^{-4}, as apparent in table 3. These conclusions are also true for the DH approximation.

Table 3. Minus the dimensionless energy $\beta u_N(\Gamma)/\Gamma$ of the OCP as a function of Γ for MC (with error bars), HNC, Cohen and Ortner approximations.

Γ	MC	HNC	Cohen	Ortner
0.1	0.251 17(34)	0.256 885 48	0.256 772 26	0.256 991 74
0.2	0.341 11(17)	0.342 389 29	0.341 273 38	0.344 368 59
0.3	0.397 693(64)	0.398 377 11	0.396 081 73	0.407 617 77
0.4	0.439 323(53)	0.439 682 53	0.441 155 47	0.464 322 08
0.5	0.472 172(42)	0.472 084 81	0.493 023 26	0.521 520 956
0.6	0.498 715(21)	0.498 506 18	0.571 443 85	0.585 657 11
0.7	0.521 064(20)	0.520 642 02	0.701 204 87	0.672 444 93
0.8	0.540 173(15)	0.539 565 86	0.912 765 40	0.819 963 38
0.9	0.556 823(30)	0.556 000 50	1.242 5017	1.105 3739
1.0	0.571 403(24)	0.570 455 34	1.732 7877	1.665 1877

- The agreement between HNC energies and that predicted by Cohen *et al* expression (cf 'Th1' in figure 3 and table 3) differs by less than 2×10^{-3} in the range $0 \leqslant \Gamma \leqslant 0.3$. Note that the apparent discrepancies between the p_i of the fit of HNC and the 'exact' coefficients of Cohen expansion do not spoil the excellent agreement between the two approaches.
- The agreement between HNC energies and that predicted by Ortner *et al* expression (cf 'Th2' in figure 3 and table 3) differ by less than 2×10^{-3} in the range $0 \leqslant \Gamma \leqslant 0.2$.

From these remarks we conclude that HNC is, as expected, exact in the low coupling regime at least up to $\Gamma = 0.3$. Moreover, DH theory cannot be trusted for $\Gamma \geqslant 0.1$, Cohen *et al* expression can be used confidently as it stands for $\Gamma \leqslant 0.3$ and, unexpectedly, the additional orders in the asymptotic expression obtained by Ortner do not improve, unfortunately, on Cohen results. We suggest to reexamine the details of the calculations of reference [4].

2.3. MC theoretical background

MC simulations are not well adapted to the low coupling regime for two reasons. First, since the differences between the configurational energies of the Markov chain are small, nearly all the *a priori* displacements of particles are accepted and the convergence of the MC process is slow. Secondly, in the case of the OCP considered here, the Debye length $\lambda_D = 1/\sqrt{3\Gamma}$ diverges as $\Gamma \to 0$ and thus becomes larger than the (finite) size of the simulation box, which entails severe finite size effects. To use the MC method for obtaining very precise results for the OCP in the range of $0 \leqslant \Gamma \leqslant 1$ is therefore a real challenge. Some comments on our methodology seem to us worthwhile.

Our simulations were performed in the canonical ensemble within hyperspherical boundary conditions. The particles are thus confined on the surface of a $4D$ sphere $\mathcal{S}^3$ of radius R, and the plasma pair potential between ions is simply the Coulombic interaction in this geometry. The latter has a simple analytical expression and can thus be evaluated with an arbitrarily high precision (we used a tabulation on 50 000 points with a quadratic Hermitte interpolation and an overall precision of $\sim 10^{-9}$ on the pair interaction). This allows high-precision computations in contrast with the usual technique of Ewald summations where the potential is poorly determined at short distances which entails a precision which does not exceed $\sim 10^{-5}$ (see the discussion of [18] for instance). The theoretical background of this method has been already addressed in detail in [10, 11] and will not be rediscussed here. We

only extract from these previous theoretical considerations the following point. It turns out that the DH equation (i.e. Helmoltz equation) can be solved analytically in $\mathcal{S}^3$ which yields the exact finite size dependence of the excess internal energy in this approximation and therefore in the low coupling limit. One finds that at the leading order

$$u_N(\Gamma) - u_\infty(\Gamma) \sim N^{-2/3} \qquad \text{for} \qquad \Gamma \to 0 \qquad \text{and} \qquad N \to \infty. \tag{2.4}$$

Of course this behaviour in only asymptotic and sub-leading terms in $[N^{-2/3}]^2$, $[N^{-2/3}]^3$ must be taken into account if N is not large enough. For couplings $\Gamma \geqslant 3$, we have shown in paper I that we rather have $u_N(\Gamma) - u_\infty(\Gamma) \sim N^{-1}$. This remark yields the correct procedure: for a given parameter Γ, perform MC simulations for different number of particles N and take advantage of the scaling relation (2.4) to obtain the thermodynamic limit $u_\infty(\Gamma)$. The estimation of the statistical errors on the $u_N(\Gamma)$ and the extrapolated thermodynamic limit $u_\infty(\Gamma)$ is also described in detail in I. However, by contrast with [10, 11] devoted to the strong correlation regime ($1 \leqslant \Gamma \leqslant 190$), in the present work only the small couplings are considered. In order to test the validity of HNC, notably in the range $0.3 \leqslant \Gamma \leqslant 1$ with an error of $\sim 1 \times 10^{-4}$, we were led to perform huge Markov chains and consider very large systems up to $N = 51\,200$ particles in order to reach the scaling region where (2.4) applies. Since HNC and Cohen asymptotic forms for u differ by less than $\sim 1 \times 10^{-4}$ in the range $0 \leqslant \Gamma \leqslant 0.3$, we can claim (as will be discussed in detail below) an overall maximum error of $\sim 1 \times 10^{-4}$ for the dimensionless $\beta u/\Gamma$ in the whole interval $0 \leqslant \Gamma \leqslant 1$.

Some additional simulations in the transition region to a high correlation regime $1 \leqslant \Gamma \leqslant 10$ were also performed to make a contact with our previous results.

3. MC data analysis and fits

3.1. Data analysis

We adopted the same procedure as the one described in reference I. The MC simulations were performed using the standard Metropolis algorithm to build Markov chains in the canonical ensemble. In the small Γ regime, $0 \leqslant \Gamma \leqslant 1$, where finite size effects are tremendously important, we considered much larger systems than before. In order to get the thermodynamic limit (TL) of the excess internal energy for each value of Γ, we performed simulations for samples of $N = 100, 200, 400, 800, 1600, 3200, 6400, 12\,800, 25\,600$ and $51\,200$ particles. The cumulated reduced excess energy (CREE) $\beta U(\Gamma, N)/\Gamma$, at coupling Γ and number of particles N, was computed as the cumulated mean over M successive configurations 'i' of the Markov chains as

$$\frac{\beta u_{N,\Gamma}(M)}{\Gamma} = \frac{1}{M}\sum_{i=1}^{M} \frac{\beta V(i)}{N\Gamma} \quad (1 \leqslant M \leqslant n_{\text{nconf}}). \tag{3.1}$$

We generated MC chains of $n_{\text{nconf}} = 4 \times 10^9$ configurations after thermal equilibration, for all systems up to $N = 25\,600$ particles. The reason was to reach a stable plateau for the CREE and to reduce statistical errors. These two points will be illustrated further. For $N = 25\,600$, such long chains result in the mixing of five independent chains, each one corresponding to half a month of CPU time. Thus, the $N = 25\,600$ value of the excess energy represents a 2 month and a half calculation. For $N = 12\,800$, the total duration was 2 months, with two independent chains. For comparison, $N = 800$ simulations are performed in 2 days in a unique chain. One day is enough for $N = 400$ simulations. These calculations have been performed simultaneously on the CEA Opteron clusters, local PC and the CRI cluster of Orsay, using one processor by job.

Table 4. Minus the MC energy $\beta u_N(\Gamma)/\Gamma$ of the OCP as a function of Γ and the number of particles N. The number in bracket which corresponds to *one standard deviation* σ is the accuracy of the last digit.

Γ	$N = 1600$	$N = 3200$	$N = 6400$	$N = 12800$	$N = 25600$	$N = 51200$
0.1	0.209 42(7)	0.213 43(8)	0.219 84(8)	0.227 28(7)	0.234 36(7)	0.240 18(18)
0.2	0.320 66(7)	0.324 77(6)	0.328 65(4)	0.332 23(4)	0.335 02(4)	0.337 244(74)
0.3	0.385 447(36)	0.388 389(23)	0.391 016(23)	0.393 158(27)	0.394 704(25)	0.395 825(99)
0.4	0.430 965(23)	0.433 233(23)	0.435 009(19)	0.436 452(19)	0.437 507(18)	0.438 230(63)
0.5	0.465 821(16)	0.467 568(17)	0.468 939(17)	0.470 015(17)	0.470 754(15)	0.471 263(52)
0.6	0.493 812(13)	0.495 220(13)	0.496 352(16)	0.497 158(13)	0.497 714(13)	0.498 072(37)
0.7	0.517 109(13)	0.518 254(12)	0.519 178(12)	0.519 806(11)	0.520 259(13)	0.520 600(32)
0.8	0.536 909(8)	0.537 854(7)	0.538 606(9)	0.539 140(11)	0.539 513(11)	0.539 745(25)
0.9	0.554 034(10)	0.554 810(12)	0.555 458(8)	0.555 886(11)	0.556 232(10)	0.556 458(40)
1.0	0.569 012(15)	0.569 714(9)	0.570 281(8)	0.570 669(10)	0.570 930(9)	0.571 119(24)

In order to compute MC *statistical* errors on $\beta u_N(\Gamma)/\Gamma$, each total run was divided into n_B blocks and the error bar was obtained by a standard block analysis [20]. Each block involved a large number n_B^{conf} of successive MC configurations and was supposed to be statistically independent of the others. For each calculation we checked that the variance was independent of the size of the blocks for sufficiently large values of n_B^{conf}. Results are so stable that we shall no more discuss this point in this paper. The need of large simulations with $N = 51\,200$ particles appeared with the difficulty to reach the thermodynamic limit and to obtain the required precision for the Γ values that we considered. But due to huge demand in the CPU time of these simulations (one month for 10 000 configurations), only short chains were considered, however long enough to reach the stable plateau of the CREE and to improve the TL research (see below). Our data for $\beta u_N(\Gamma)/\Gamma$ are reported in table 4 where the number in bracket corresponds to *one standard deviation* σ and represents the accuracy of the last digits, and only the results for $N \geqslant 1600$ are given.

3.2. *Connection with former simulations for* $1 \leqslant \Gamma \leqslant 10$

Before we present our new results for $0 \leqslant \Gamma \leqslant 1$, we shall study the connection with the results obtained in paper I, calculated with the same MC code, but another range of Γ values, i.e. $\Gamma \geqslant 1$. The only difference between the two calculations, both processed in FORTRAN double precision, is thus the maximum number of configurations, typically $n_{\text{conf}} = 800 \times 10^6$ MC configurations, after equilibration, in the previous case (case 'a'), and $n_{\text{conf}} = 5 \times 10^9$ in this paper (case 'b'). We have performed comparisons for $\Gamma = 1, 2, 3, 4, 5$ and 10. The choices retained in I were, at that time, the maximum reasonable conditions for the simulations.

Finite size effects decrease with increasing value of Γ. Details of CREE's for $\Gamma = 5$ and $\Gamma = 10$ are reported in table 5 (N dependence of MC energy $\beta u_N(\Gamma)/\Gamma$ in both calculations, present and I). For $\Gamma = 10$, the results are in good agreement. But for $\Gamma = 5$, slight discrepancies observed at $N = 1600$ and $N = 3200$ between the two calculations are a bit worrying. Indeed, in these cases the error bars' intervals do not overlap. The main reason is that, for the lowest Γ results of I, the plateau of the CREE was in fact not reached.

This feature is illustrated by figure 5 where the CREE's for $\Gamma = 2$ are displayed. The figure illustrates the lack of configurations in the simulations of I for the CREE $\beta U/\Gamma$ versus the number of configurations, displayed for different numbers of particles. From top to bottom,

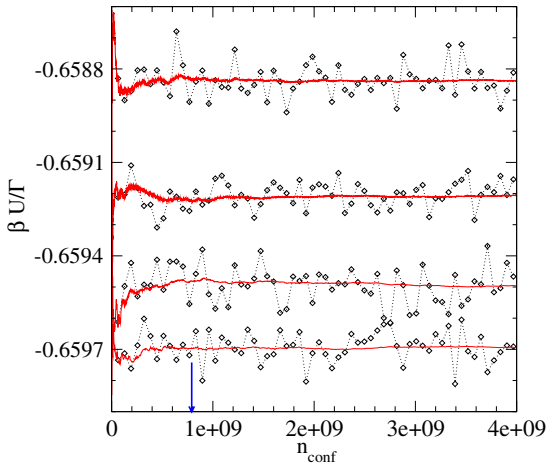

Figure 5. Solid lines: cumulated reduced excess energy $\beta u_N(\Gamma)/\Gamma$ versus the number of configurations for $\Gamma = 2$. From bottom to top $N = 800, 1600, 3200, 6400$. Symbols: block averages. The arrow points to the maximum number of configurations $n_{\rm conf} = 8 \times 10^8$ considered in I.

Table 5. Comparison with previous results of the MC energy $\beta u_N(\Gamma)/\Gamma$ of the OCP in function of the number of particles N for $\Gamma = 5$ and $\Gamma = 10$. The first row, case 'a', corresponds to the present study and the second row, case 'b', to table 1 of [11]. The only difference between the two calculations is the number of configurations, typically $n_{\rm conf} = 800 \times 10^6$ MC configurations after equilibration in case 'a', and $n_{\rm conf} = 5 \times 10^9$ in case 'b'. The number in bracket which corresponds to *one standard deviation* σ is the accuracy of the last digit. With two standard deviations the agreement is fulfilled.

Γ	$N = 400$	$N = 800$	$N = 1600$	$N = 3200$	$N = 6400$	case
5		0.751 0930(37)	0.751 1501(31)	0.751 2037(35)	0.751 2332(21)	a
5	0.751 0201(89)	0.751 1042(126)	0.751 1513(135)	0.751 1775(85)		b
10		0.799 8396(26)	0.799 8148(30)	0.799 8098(28)	0.799 8043(15)	a
10	0.799 8865(53)	0.799 8414(43)	0.799 8149(51)	0.799 8131(55)		b

$N = 800, 1600, 3200, 6400$. The arrow points to the maximum number of configurations considered in I. When compared to our new calculations, clearly the Markov chain was not long enough to reach a plateau and such a drift of the CREE was probably underestimated in our previous calculations. The large variation with N of the CREE with N (solid (red) line) gives an idea of the amplitude of finite size effects. The simulation for the case $N = 6400$, not included in paper I, has been added to improve the TL extrapolation. Only the 4×10^9 first configurations are plotted for visibility, but clearly each CREE value reaches its equilibrium value for a fixed N value. Figure 6 illustrates how the previous conclusions for the case $\Gamma = 2$ are emphasized in the case $\Gamma = 1$.

It follows from the above remarks that a re-analysis of the TL of the energy of the OCP is necessary for $\Gamma = 1, 2, \ldots, 10$. We recall the conclusions of I according to which the scaling law (2.4) is valid only for low Γ and that for $\Gamma \gtrsim 3 - 4$ the thermodynamic limit is reached more quickly with a scaling law

$$u_N(\Gamma) - u_\infty(\Gamma) \sim N^{-1} \qquad \text{for} \quad \Gamma \gtrsim 3 - 4 \qquad \text{and} \qquad N \to \infty. \tag{3.2}$$

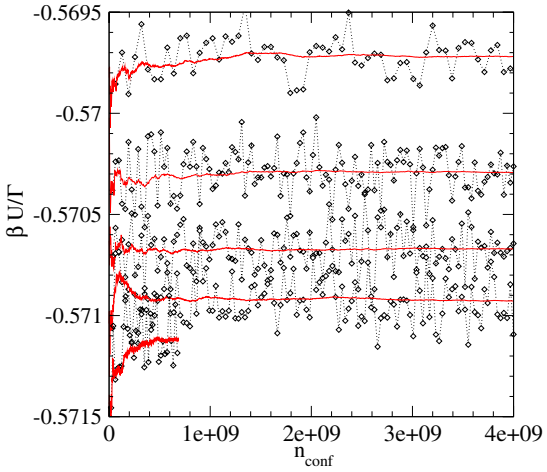

Figure 6. Solid lines: cumulated reduced excess energy $\beta u_N(\Gamma)/\Gamma$ versus the number of configurations for $\Gamma = 1$. From top to bottom $N = 3200, 6400, 12\,800, 25\,600, 51\,200$. Symbols: block averages.

Table 6. Thermodynamic limit of the energy of the OCP versus Γ, $\Gamma \geqslant 1$. First column: this work, third column: results of [11]. The type of extrapolation scheme is specified in the column 'fit'. For instance, quad(3200–51200) means that a quadratic regression involving the data from $N = 3200, 6400, 12\,800, 51\,200$ has been used. The variable entering the fit is specified in the column 'Variable'. p is the precision of the fit. The number in bracket which corresponds to *one standard deviation* σ is the accuracy of the last digit.

Γ	$\beta u_\infty/\Gamma$	Fit	$p \times 10^5$	$\beta u_\infty/\Gamma$	Fit	$p \times 10^5$	Variable
	This work			reference [11]			
1.	−0.571 387(24)	lin(12800–51200)	4.2	−0.571 098(39)	cub(100-3200)	6.9	$N^{-2/3}$
1.	−0.571 403(22)	quad(3200–51200)	3.8				$N^{-2/3}$
2.	−0.659 8934(68)	quad(800–6400)	7.0	−0.659 983(23)	quad(200-3200)	3.5	$N^{-2/3}$
3.	−0.704 2987(54)	quad(3200–6400	0.8	−0.704 348(19)	quad(200-3200)	2.7	$N^{-2/3}$
4.	−0.731 9760(46)	lin(800–6400)	0.6	−0.731 916(12)	quad(200-3200)	1.7	N^{-1}
5.	−0.751 2608(22)	lin(800–6400)	0.3	−0.751 2126(98)	quad(200-3200)	1.3	N^{-1}
10.	−0.799 7991(16)	lin(800–6400)	0.2	−0.799 7974(45)	lin(400-3200)	0.56	N^{-1}

Moreover, the scaling limits (2.4) and (3.2) are satisfied, depending on the value of Γ, for very large, and sometimes prohibitive large, numbers of particles N. The ideal case would be a linear fit passing through all the points within the error bars. This situation was indeed observed by including simulations at $N = 51\,200$ particles and for not too low values of Γ. In other situations we had to content ourselves with quadratic fits including the next leading-order term (i.e. either $\mathcal{O}(1/N^2)$ or $\mathcal{O}(1/N^{4/3})$ according to the value of Γ). In table 6, the comparisons for the TL of the energy between the present paper and results of paper I for $\Gamma = 1, 2, 3, 4, 5, 10$ are resumed. The type of the extrapolation scheme is specified in the column 'fit', together with the interval of N values considered for the fit. Precision is also reported. For $\Gamma \leqslant 5$, it is clear that results are slightly shifted between calculations. As expected for $\Gamma = 10$, the present results and those of [11] are similar; higher values of Γ should not cause any trouble.

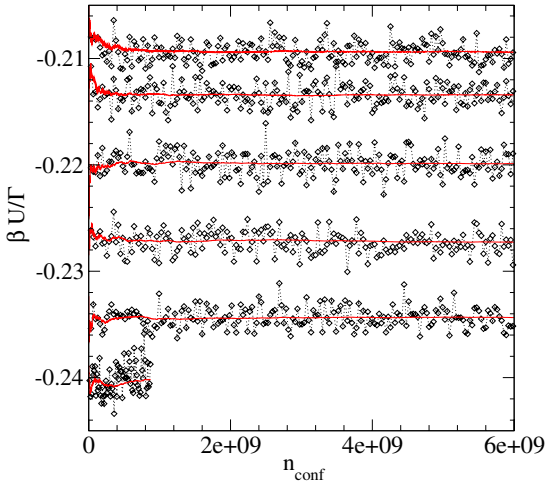

Figure 7. Solid lines: cumulated reduced excess energy $\beta u_N(\Gamma)/\Gamma$ versus the number of configurations for $\Gamma = 0.1$. From top to bottom $N = 1600, 3200, 6400, 12\,800, 25\,600, 51\,200$. Symbols: block averages.

3.3. Thermodynamic limit extrapolation scheme

The aim of our simulations was to compute the TL of the energy $\beta u_{N=\infty}(\Gamma)$ with a high degree of accuracy by taking into account finite size effects which are of overwhelming importance for $\Gamma \leqslant 1$. The need of simulations up to $N = 51\,200$ and involving no less than $N = 800$, or even $N = 1600$ particles for the smallest values of Γ, appeared crucial to reach the scaling law (2.4). It appears that, for this range of N, MC data can be fitted with the quadratic fits:

$$\beta u_N(\Gamma) = \beta u_{N=\infty}(\Gamma) + a_1 \frac{1}{N^{2/3}} + a_2 \left[\frac{1}{N^{2/3}}\right]^2 . \tag{3.3}$$

For most values of Γ, it proved possible to explicitly check the asymptotic form linear in $N^{-2/3}$ (i.e. $a_2 = 0$ in equation (3.3)) by keeping only the three largest systems, i.e. $N = 12\,800, 25\,600$ and $51\,200$. Recall that in paper I the largest considered systems were made of $N = 3200$ particles. An exhaustive discussion follows in the next section.

3.4. Results for $0 \leqslant \Gamma \leqslant 1$

We present and discuss in detail the ten values $\Gamma = 0.1, 0.2, \ldots, 1$ considered in our numerical experiments. Figures 7, 8, 9 and 10 illustrate the CREE $\beta u_N(\Gamma)/\Gamma$ versus the number of configurations for several characteristic values of Γ($\Gamma = 0.1$, 0.2, 0.4 and 0.7 respectively) typical of the different plasma regimes in the interval $(0, 1)$. Our previous comments on figures 6 and 5 (for $\Gamma = 1, 2$ respectively) are still valid in these cases. We stress once again the need of large systems together with the need of enough configurations to reach a stable plateau after thermal equilibration.

All generated configurations, $n_{\text{conf}} = 6 \times 10^9$, are displayed in figure 7 ($\Gamma = 0.1$) while a zoom of only the first 2×10^9 configurations is displayed in figure 8 ($\Gamma = 0.2$), which exemplifies the plateau reached by the CREE for $N = 51\,200$. In the last two figures 9 and 10, respectively, for $\Gamma = 0.4$ and $\Gamma = 0.7$ and $n_{\text{conf}} = 4 \times 10^9$, we see the good convergence with N as the interval width between CREE values decreases from top to bottom. By contrast,

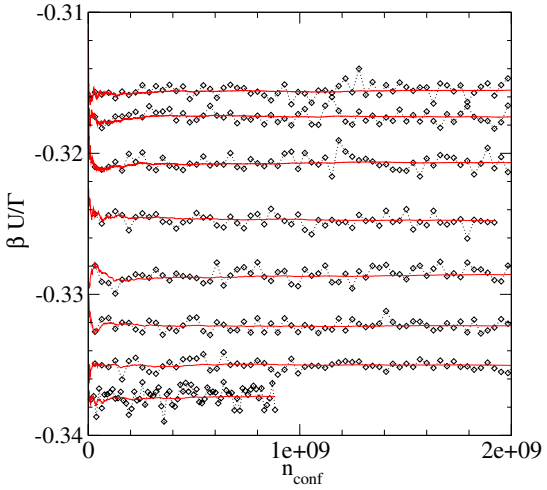

Figure 8. Solid lines: cumulated reduced excess energy $\beta u_N(\Gamma)/\Gamma$ versus the number of configurations for $\Gamma = 0.2$. From top to bottom $N = 400, 800, 1600, 3200, 6400, 12\,800, 25\,600, 51\,200$. Symbols: block averages.

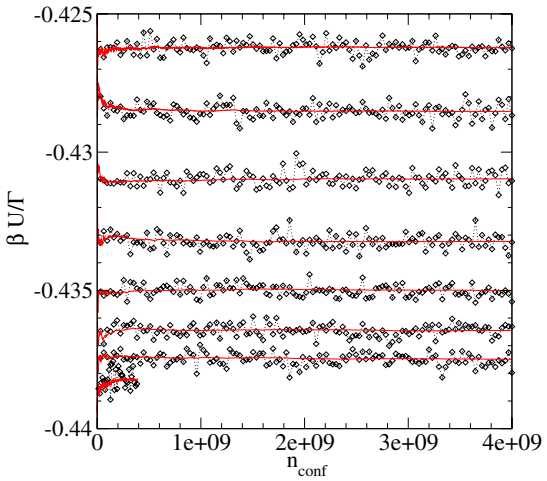

Figure 9. Solid lines: cumulated reduced excess energy $\beta u_N(\Gamma)/\Gamma$ versus the number of configurations for $\Gamma = 0.4$. From top to bottom $N = 400, 800, 1600, 3200, 6400, 12\,800, 25\,600, 51\,200$. Symbols: block averages.

the low Γ runs do not exhibit this regular decrease. Of course beyond visual impressions only the possibility and precision of the fitting process of the MC CREE results will give a firm answer on the quality of the TL calculation for each Γ value.

Table 4 resumes the present work MC calculations of the MC energy $\beta u_N(\Gamma)/\Gamma$ of the OCP as a function of Γ for $N = 1600$ to $N = 51\,200$. The number in bracket which corresponds to *one standard deviation* σ is the accuracy of the last digit. Results corresponding to $N \leqslant 1600$, not included in the fits, are not reported. The thermodynamic limit values of the energy versus Γ are reported in table 7. The type of extrapolation schemes retained in the

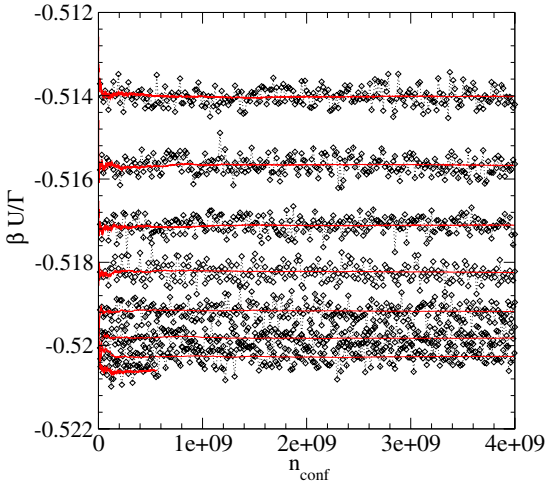

Figure 10. Solid lines: cumulated reduced excess energy $\beta u_N(\Gamma)/\Gamma$ versus the number of configurations for $\Gamma = 0.7$. From top to bottom $N = 400, 800, 1600, 3200, 6400, 12\,800, 25\,600, 51\,200$. Symbols: block averages.

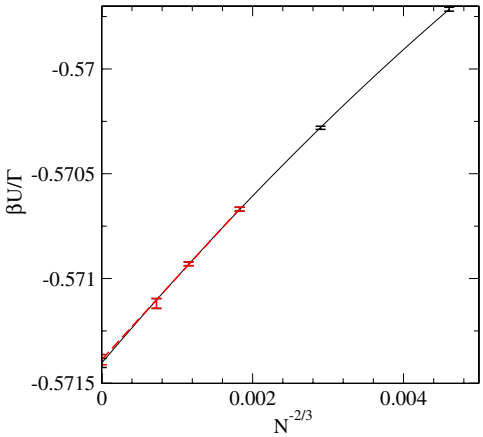

Figure 11. Solid lines: cumulated reduced excess energy $\beta u_N(\Gamma)/\Gamma$ versus $1/N^{2/3}$ for $\Gamma = 1$. From left to right $N = \infty, 51\,200, 25\,600, 12\,800, 6400, 3200$. At finite N, the error bars correspond to one standard deviation σ on the MC data. The error bar on the TL limit ($N = \infty$) is computed by the regression. Solid black line: quadratic polynomial regression. Dashed line: linear regression for the three larger values of N.

fits, i.e. linear or quadratic (cf equation (3.3)), are specified. In figures 11, 12, 13 and 14 we display the quadratic fit of $\beta u_N(\Gamma)/\Gamma$ (solid black line) and the linear fits for the three largest numbers of particles considered, when available ((red) dashed line) for $\Gamma = 1, 0.7, 0.4\,\Gamma = 0.1$ respectively. The error bars on the value of the TL of the energy $\beta u_\infty(\Gamma)/\Gamma$ reported in table 7 are the error bars of the linear (or quadratic) regression.

We discuss now the results from high to low Γ's. Figure 11 illustrates the high quality of the fits obtained in the case $\Gamma = 1.0$. Indeed, the extrapolated TL of $\beta u_N(\Gamma)/\Gamma$ coincide for both the linear and the quadratic fits (the latter involving more states with a low number of

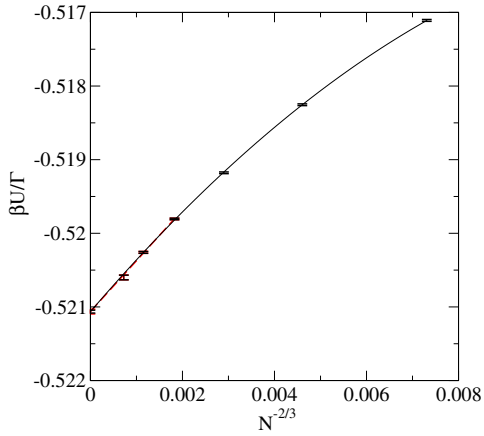

Figure 12. Same legend as figure 11 but for $\Gamma = 0.7$. From left to right $N = \infty, 51\,200$, 25 600, 12 800, 6400, 3200, 1600.

Table 7. Thermodynamic limit of the energy of the OCP versus Γ. The number in bracket which corresponds to *one standard deviation* σ is the accuracy of the last digit. The type of extrapolation scheme is specified in the column 'fit'. For instance, quad(3200–51 200) means that a quadratic regression involving the data from $N = 3200, 6400, 12\,800, 51\,200$ has been used. The variable entering the fit is $N^{-2/3}$.

Γ	$\beta u_\infty / \Gamma$	Fit
0.1	−0.251 17(34)	quad(6400–51200)
0.2	−0.341 11(17)	quad(6400–51200)
0.3	−0.397 693(64)	quad(3200–51200)
0.4	−0.439 323(53)	lin(12800–51200)
0.4	−0.439 528(50)	quad(3200–51200)
0.5	−0.472 028(45)	lin(12800–51200)
0.5	−0.472 172(42)	quad(3200–51200)
0.6	−0.498 663(38)	lin(12800–51200)
0.6	−0.498 715(21)	quad(1600–51200)
0.7	−0.521 063(32)	lin(12800–51200)
0.7	−0.521 064(20)	quad(1600–51200)
0.8	−0.540 146(28)	lin(12800–51200)
0.8	−0.540 173(15)	quad(1600–51200)
0.9	−0.556 823(30)	lin(12800–51200)
0.9	−0.556 801(25)	quad(3200–51200)
1.0	−0.571 387(24)	lin(12800–51200)
1.0	−0.571 403(22)	quad(3200–51200)

particles and the former only the three largest systems) with a nice overlap of the error bars. Results are similar down to $\Gamma = 0.7$, as illustrated in figure 12 for $\Gamma = 0.7$.

In the range $0.5 \leqslant \Gamma \leqslant 0.7$ the precision of the fits is good but the linear and the quadratic fit extrapolations do not give exactly the same TL values; however, the error bars do overlap. Figure 13, corresponding to the case $\Gamma = 0.4$, illustrates the smallest Γ at which a linear fit is possible with the three higher values of N. The linear and the quadratic fit extrapolations

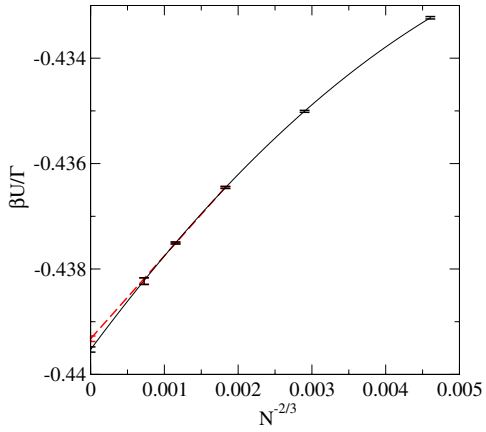

Figure 13. Same legend as figure 11 but for $\Gamma = 0.4$. From left to right $N = \infty$, 51 200, 25 600, 12 800, 6400, 3200.

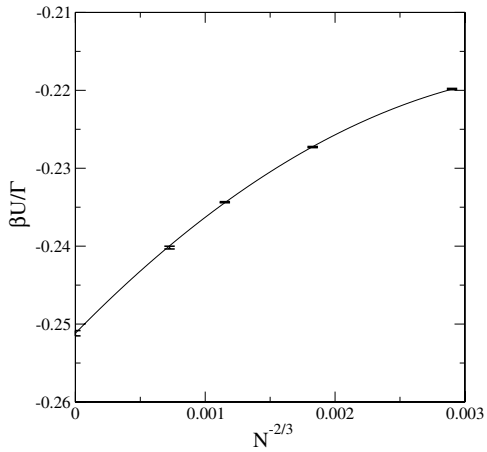

Figure 14. Solid lines: cumulated reduced excess energy $\beta u_N(\Gamma)/\Gamma$ versus $1/N^{2/3}$ for $\Gamma = 0.1$. From left to right $N = \infty$, 51 200, 25 600, 12 800, 6400, 3200. The error bars correspond to one standard deviation σ. Solid black line : quadratic polynomial regression of MC data.

giving the TL values would coincide within the error bars if the latter were defined to be *two standard deviations* rather than only *one* according to our choice.

For Γ smaller or equal to 0.3, it was impossible to reach an asymptotic form of $\beta u_N(\Gamma)/\Gamma$, linear in the variable $N^{-2/3}$, and only a quadratic polynomial fit was possible (cf table 7). For that reason it is legitimate to consider the error bars on the extrapolated value $\beta u_\infty(\Gamma)/\Gamma$ as overoptimistic in this range of Γ, see figure 14 for an illustration in the case $\Gamma = 0.1$. Simulations involving larger number of particles would be necessary but are out of our reach.

For all the states with a $\Gamma \geqslant 0.4$, the TL limit $u_\infty(\Gamma)$ can thus be obtained with a high precision, $p \sim 10^{-5}$, after a careful study of finite size effects on the MC energies $u_N(\Gamma)$. For smaller values of Γ, for instance $\Gamma = 0.1$, samples of more than $N \simeq 200\,000$ particles should be used to reach the leading order of the asymptotic regime (2.4). However, such an effort

would be useless since HNC and Cohen approximations are then 'exact' within the required precision on u. The $u_\infty(\Gamma)$ are perfectly well fitted in the range $0.4 \leqslant \Gamma \leqslant 1$ by the Cohen's functional form, given by equation (2.1*a*), involving the five parameters p_i ($i = 0, \ldots, 4$) given in table 1. We notice large differences between these parameters and those obtained for HNC but we recall that the latter reproduce HNC data in a different range, i.e. $0 \leqslant \Gamma \leqslant 1$.

4. Conclusion

In this conclusion we compare at first the Cohen–Ortner low Γ expansions, HNC and MC data. Figure 3 shows without ambiguity the good agreement between HNC and MC results in the range $0 \leqslant \Gamma \leqslant 1$ and the large departure of both results with analytical expansion ones, DH (for $\Gamma \geqslant 0.05$), Th1 (for $\Gamma \geqslant 0.3$) and Th2 (for $\Gamma \geqslant 0.2$). Note however that the scale of the figure is not large enough to discriminate between HNC and MC results, notably because the error bars on MC results are smaller than the size of the symbols. A more enlightening illustration is that of figure 2 which gives the ratio of the MC and HNC energies. The disagreement for $\Gamma \leqslant 0.3$ results from a bad evaluation of the TL of u_N due to huge finite size effects spoiling the MC data, while the disagreement for $\Gamma \geqslant 0.6$ simply reflects the failure of the HNC approximation at high Γ. A nearly perfect agreement between MC and HNC results, compatible with *one standard deviation*, is observed only at $\Gamma = 0.5$; with *two standard deviations* the HNC results are within the error bars of the MC data in the interval $0.4 \leqslant \Gamma \leqslant 0.6$. By passing, our new HNC calculations for some values of Γ in the range $(1, 10)$ are plotted in figure 4 where MC data were also included for comparison.

It is the place to resume our analysis. We found that, for a required precision of $p = 10^{-5}$ on the energy,

- $0 \leqslant \Gamma \leqslant 0.05$ is the range of validity of Debye–Hückel theory.
- $0 \leqslant \Gamma \leqslant 0.3$ is the range of validity of Cohen low Γ expansion (2.1).
- Ortner's additional terms do not improve the results.
- $0 \leqslant \Gamma \leqslant 0.5$ is the range of validity of HNC. The data are perfectly represented by the eight parameters fit of tables 1 and 2.
- We were able to extract the thermodynamic limit of the OCP energy from our MC simulations with a precision not smaller than $p = 10^{-5}$ in the range $0.4 \leqslant \Gamma \leqslant 1$. Our data are well fitted by the five parameters fit of table 1.

Admittedly 43 years after the seminal paper of SG Brush, HL Sahlin and E Teller [6], we produce results which differ within only a few percent but these few percents are the price to pay to assess the validity of the various analytical predictions and provide reference data of the OCP equation of state.

References

[1] Baus M and Hansen J-P 1980 *Phys. Rep.* **59** 1
[2] Debye P E and Hückel E 1923 *Physikalische Zeitschrift* **24** 185
[3] Cohen E G D and Murphy T J 1969 *Phys. Fluids* **12** 1404
[4] Ortner J 1999 *Phys. Rev.* E **59** 6312
[5] Ng K-C 1974 *J. Chem. Phys.* **61** 2680
[6] Brush S G, Sahlin H L and Teller E 1966 *J. Chem. Phys.* **45** 2102
[7] Pollock E L and Hansen J P 1973 *Phys. Rev.* A **8** 3110
[8] Slattery W L, Doolen G D and DeWitt H E 1982 *Phys. Rev.* A **26** 2255
[9] De Witt H E 1997 *Proc. of the Int. Conf. on Strongly Coupled Coulomb Systems* (Boston)
[10] Caillol J-M 1999 *J. Chem. Phys.* **111** 6528
[11] Caillol J-M 1999 *J. Chem. Phys.* **111** 6538

[12] Caillol J-M and Gilles D 2003 *J. Phys. A: Math. Gen.* **36** 6243
[13] Potekhin A Y and Chabrier G 2000 *Phys. Rev.* E **62** 8554
[14] Caillol J-M and Gilles D 2000 *J. Stat. Phys.* **100** 933
[15] Stratonovich R L 1958 *Sov. Phys. Solid State* **2** 1824
[16] Hubbard J 1954 *Phys. Rev. Lett.* **3** 77
Hubbard J and Shofield P 1972 *Phys. Lett.* A **40** 245
[17] Caillol J-M and Raimbault J L 2001 *J. Stat. Phys.* **103** 753
[18] Salin G and Caillol J-M 2000 *J. Chem. Phys.* **113** 10459
[19] Stillinger F H and Lovett R 1968 *J. Chem. Phys.* **49** 1991
[20] Frenkel D and Smit B 1996 *Understanding Molecular Simulation* (New York: Academic)